Network Spreading from Network Dimension

Jack Murdoch Moore [1,2] Michael Small [3,4] Gang Yan [1,2] Huijie Yang [5] Changgui Gu [5] and Haiying Wang [5,*]

[1]*MOE Key Laboratory of Advanced Micro-Structured Materials, and School of Physical Science and Engineering,*
Tongji University, Shanghai 200092, People's Republic of China
[2]*National Key Laboratory of Autonomous Intelligent Unmanned Systems,*
MOE Frontiers Science Center for Intelligent Autonomous Systems, Tongji University,
Shanghai 200092, People's Republic of China
[3]*Complex Systems Group, Department of Mathematics and Statistics, University of Western Australia,*
Crawley 6009, Western Australia, Australia
[4]*Mineral Resources, CSIRO, Kensington 6151, Western Australia, Australia*
[5]*Business School, University of Shanghai for Science and Technology,*
334 Jungong Road, Shanghai 200093, People's Republic of China

Continuous-state network spreading models provide critical numerical and analytic insights into transmission processes in epidemiology, rumor propagation, knowledge dissemination, and many other areas. Most of these models reflect only local features such as adjacency, degree, and transitivity, so can exhibit substantial error in the presence of global correlations typical of empirical networks. Here, we propose mitigating this limitation via a network property ideally suited to capturing spreading. This is the network correlation dimension, which characterizes how the number of nodes within range of a source typically scales with distance. Applying the approach to susceptible-infected-recovered processes leads to a spreading model which, for a wide range of networks and epidemic parameters, can provide more accurate predictions of the early stages of a spreading process than important established models of substantially higher complexity. In addition, the proposed model leads to a basic reproduction number that provides information about the final state not available from popular established models.

From information on social networks [1,2] and knowledge in organizations [3] to diseases across the globe [4,5], the modern human experience is governed by spreading on networks. Among our most important tools for understanding spreading processes are continuous-state network spreading models [2–18], which capture discrete and random spreading process using continuous deterministic variables representing the expected outcomes over many realisations. However, many of these models are limited by their reliance on local features, such as degree [9], degree correlations [10], transitivity [11], or adjacency [12–17], which can only represent each node's immediate neighborhood and reflect just one or two of the immediately succeeding transmission steps. They achieve excellent performance on graphs satisfying the appropriate mixing assumptions, but may be challenged by more realistic structures [19–22].

Spreading is a dynamical process which expands from microscopic to macroscopic structural scales. The spreading process reflects structure on multiple scales, and spreading models should do the same. Here we consider accommodating multiple scales via network dimension, which captures structural self-similarity and in recent years has been increasingly utilized to characterize specific aspects of spreading processes [23–26] and to identify influential disseminators [27,28]. Specifically, we consider network correlation dimension, which uses a power-law model to characterize how the number of nodes within range of a source typically scales with distance and has been shown to capture the structure of many empirical networks [29–31]. We formulate a model for susceptible-infected-recovered (SIR) processes which depends on only three topological parameters other than network size: mean degree, network correlation dimension and a constant of proportionality. We show that, compared with important established models of substantially higher parametric complexity, for a wide range of synthetic and empirical networks our model provides better characterization of early spreading and leads to a basic reproduction number which supplies additional information about the final system state. Example code is available in Ref. [32].

Dimensional spreading model.—We demonstrate the capacity of network dimension to capture spreading by considering an SIR process, forms of which have been

used to model diverse phenomena [33] including, e.g., the spread of rumours [34], information [35], computer viruses [36], and interest in stocks [37]. In each time step, an infected node enters the recovered state with probability $\gamma \in [0, 1]$, while a susceptible node with an infected neighbor enters the infected state with probability $\lambda \in [0, 1]$.

The dimensional spreading model for the number $S(t)$, $I(t)$, and $R(t)$ of susceptible, infected, and recovered nodes at time t is defined by the difference equations

$$S(t + 1) = S(t) - \nu(t),$$
$$I(t + 1) = I(t) + \nu(t) - \gamma I(t), \qquad (1)$$

together with the condition $S(t) + I(t) + R(t) = N$, where N is the size of the network. In Fig. 1 we illustrate the first part of the proposed method to determine the number $\nu(t)$ of newly infected nodes. To estimate the network distance r the infection has spread, we model the mean number of nodes at network distance r as

$$u(r) = \alpha r^{D-1}, \qquad 1 \le r \le r_{\max}, \qquad (2)$$

where D is network correlation dimension, α is a proportionality factor, and $r_{\max}$ is the upper cutoff of the considered dimension-based structural model (see Supplemental Material [38], Sec. I). Assuming the affected region, which comprises all infected and recovered nodes, has spread to comprise a ball centered at the original spreading source, the mean over all possible origins of its size is $I + R = 1 + \sum_{s=1}^{r} \alpha r^{D-1}$. Approximating the sum as an integral, we have

$$I + R - 1 = \int_{\frac{1}{2}}^{r+\frac{1}{2}} \alpha s^{D-1} \, ds = \frac{\alpha}{D}\left(\left(r + \frac{1}{2}\right)^D - \frac{1}{2^D}\right).$$

Inverting this equation yields the radius of the infected region as

$$r = \left(\frac{D}{\alpha}(I + R - 1) + \frac{1}{2^D}\right)^{1/D} - \frac{1}{2}, \qquad (3)$$

which we will treat as a continuous-valued variable. Knowing r, we can estimate the number of nodes exposed to infection ν. These nodes must be at radius $r + 1$ so, by Eq. (2), an upper bound for the expected number of newly infected nodes is $\tilde{\nu} = \lambda \alpha (r + 1)^{D-1}$. We can then estimate the number of newly infected nodes ν by multiplying $\tilde{\nu}$ by the fraction of nodes at radius $r + 1$ which have an infected neighbor. Writing a for the fraction of nodes at radius r which are infected and b for the number of edges which a node at radius $r + 1$ typically shares with nodes in the affected region, we therefore have

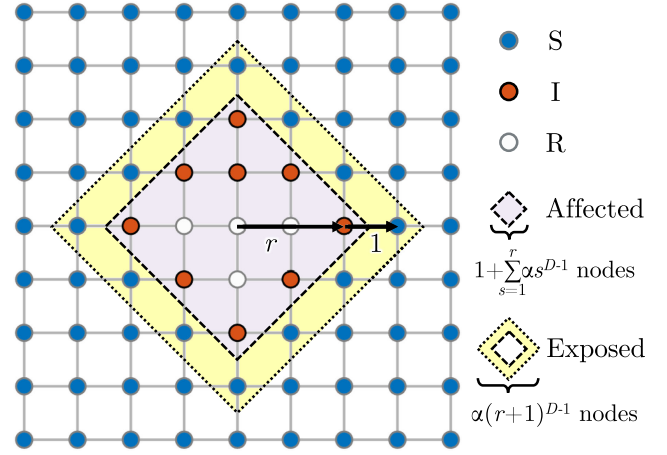$$\nu = \lambda \alpha [1 - (1 - a)^b](r + 1)^{D-1}, \qquad (4)$$

FIG. 1. Network geometry determines how a quantity spreads from its source. Basis of proposed SIR dimensional spreading model: The affected region (purple square) comprises all infected (I) and recovered (R) nodes, and in a network of dimension D has volume $1 + \sum_{s=1}^{r} \alpha s^{D-1}$, where α is a proportionality factor and r is radius. All nodes exposed to infection are among the $\alpha(r + 1)^{D-1}$ susceptible (S) nodes (yellow ring) which neighbor the boundary of the affected region.

where we have assumed perfect mixing between nodes at radii r and $r + 1$. The expected fraction a will lie somewhere between $I/(I + R)$ [24] and $\min\{1, I/u(r)\}$. Using the upper bound for a, which will be valid in the early stages of spreading when λ is large compared with γ, together with Eq. (2), gives

$$a = \min\{1, I/(\alpha r^{D-1})\}. \qquad (5)$$

To estimate b we note that a node at radius $r + 1$ must have at least one neighbor at radius r, and assume that other edges are distributed randomly among nodes at radius between r and $r + 2$. With Eq. (2), this leads to

$$b = 1 + \frac{(\langle k \rangle - 1)u(r)}{\sum_{m=0}^{2} u(r + m)} = 1 + \frac{\langle k \rangle - 1}{\sum_{m=0}^{2}(1 + r^{-1}m)^{D-1}}. \qquad (6)$$

Basic reproduction number.—Having defined the dimensional spreading model, next we determine its basic reproduction number R_0, which is used to predict whether an infinitesimal level of infection will initially increase. To resolve this quantity, we apply the continuous-time approximation $(dI/dt) \approx I(t + 1) - I(t) = \mathcal{F} - \mathcal{G}$, where $\mathcal{F} = \nu(t)$ is the rate at which infections arise and $\mathcal{G} = \gamma I(t)$ is the rate at which they disappear. The next generation matrix [39] method gives the basic reproduction number at a disease-free equilibrium as

$$R_0 = \rho\left(\frac{\partial \mathcal{F}}{\partial I}\frac{\partial \mathcal{G}^{-1}}{\partial I}\right) = \frac{1}{\gamma}\rho\left(\frac{\partial \nu}{\partial I}\right),$$

where $\rho(\cdot)$ represents spectral radius. At a disease free equilibrium, where $I = 0$, by Eq. (4), (5), $R_0 = (\lambda/\gamma)b(1 + r^{-1})^{D-1}$. For $r = 0$, this expression for R_0 diverges. We instead consider $r = 1$ where, by Eq. (6),

$$R_0 = \frac{\lambda}{\gamma}\left(1 + \frac{\langle k \rangle - 1}{1 + 2^{D-1} + 3^{D-1}}\right)2^{D-1}, \qquad (7)$$

which we note is independent of α. It is straightforward to check directly that if $R_0 < 1$ ($R_0 > 1$) then an infinitesimal level of infection will initially decrease (increase) (see Supplemental Material [38], Sec. II).

Results and discussion.—Here we illustrate the ability of our model to capture epidemic spreading processes on a wide range of synthetic and empirical networks. To show the advantages of our approach, we compare it with three other continuous-state deterministic models also designed to approximate the average over many realizations of a stochastic process having discrete states. These three benchmark models have been chosen to span a wide range of complexities: homogeneous mean field (MF) is specified by two state variables and one topological free parameter; heterogeneous MF [9] is specified by $2|\mathcal{K}|$ state variables and $(|\mathcal{K}| - 1)$ topological parameters, where $\mathcal{K}$ is the set of observed node degrees; and probabilistic discrete Markov chain (PDMC) is specified by $2N$ state variables and $\langle k \rangle N/2$ topological parameters (for details on these models and some of the assumptions they employ, see Supplemental Material [38], Sec. III, and Refs. [40,41] therein). This range of complexities bounds comfortably the complexity of the proposed dimensional spreading system which, given N, is specified by two dynamical state variables, I and R, and three intrinsic topological properties, $\langle k \rangle$, D, and α.

Now we show that our model often provides a better description of the initial period of epidemic spreading. For this, we consider the time span $0 \leq t \leq t_{\max}$, where $t = 0$ is when a randomly chosen node is infected in an otherwise susceptible population, and $t_{\max}$ is the final time for which there still exist infected nodes and the dimension-based structural model given by Eq. (2) can be used to estimate the number of nodes at radius $r + 1$. For each considered network we take the true average state as the mean over 100 instances of the spreading process, each with a randomly chosen initially infected node (for details on simulations see Supplemental Material [38], Sec. IV).

To showcase the versatility of the dimensional spreading model, in Fig. 2 we apply it across a selection of networks spanning size from $N = 1152$ to $N = 62917$, correlation dimension $D = 2.00$ to $D = 6.35$, and upper cutoffs $r_{\max}$ covering the set $\{4, 6, 12, 49\}$ (for details see Supplemental Material [38], Table S1, and Refs. [42–48] therein), using $\lambda = 0.1$, $\gamma = 0.05$. For each network we track the time evolution of the fraction R/N of the population which has passed through the complete
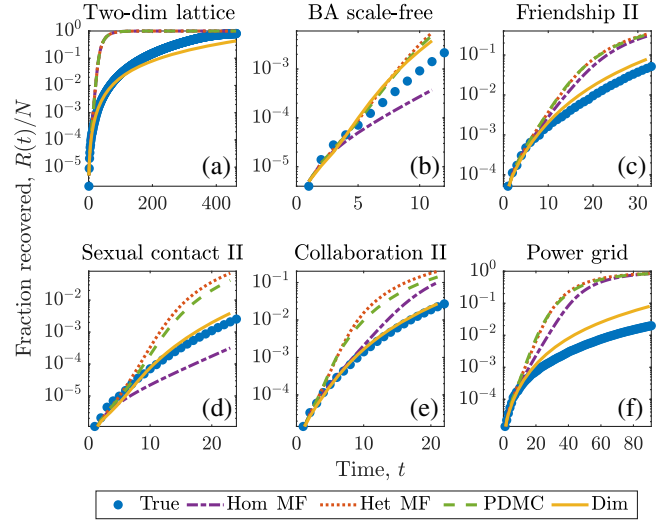

FIG. 2. The dimensional spreading model better represents early spreading on a range of synthetic and empirical networks. Spread of infection on (a) Two-dimensional lattice; (b) BA scale-free network; (c) Network of friendships between students in a high school; (d) Sexual contact network; (e) Erdős collaboration network; and (f) Power grid of the western United States. Curves represent the true mean state (filled blue circles) and estimates from homogeneous mean field (purple dot-dashed), heterogeneous mean field (red dotted), probabilistic discrete Markov chain (green dashed), and dimensional spreading model (yellow solid).

transmission cycle. Unsurprisingly, on a regular lattice, our model provides best performance [Fig. 2(a)]. Encouragingly, the proposed model is also competitive on a Barabàsi-Albert (BA) scale-free network [49] over the relatively short time interval for which a dimension-based structural model is predicted to be valid [Fig. 2(b)]. Similarly, the dimensional spreading model is the best predictor of average system evolution on two empirical networks of great relevance to disease transmission: friendships within a high school, and a sexual contact network [Figs. 2(c) and 2(d)]. Our model is also optimal for a collaboration network, pertinent to the transmission of knowledge [Fig. 2(e)], as well as a power grid germane to the cascade of electrical failures [Fig. 2(f)]. In the examples shown, heterogeneous MF and PDMC consistently overestimate the initial rate of progress, while homogeneous MF can either overestimate or underestimate. The dimensional spreading model can ameliorate these deviations, and over much of the time interval is, among all predictions, either the tightest upper bound or the closest lower bound to the true system average. The proposed model often exhibits similar advantages for the variables S, I (see Supplemental Material [38], Fig. S2), for other choices of dynamical parameters (see Supplemental Material [38], Fig. S3), for a range of other empirical networks (Fig. S4, Table S1 in [38], and Refs. [50–60] therein), and also in comparison to
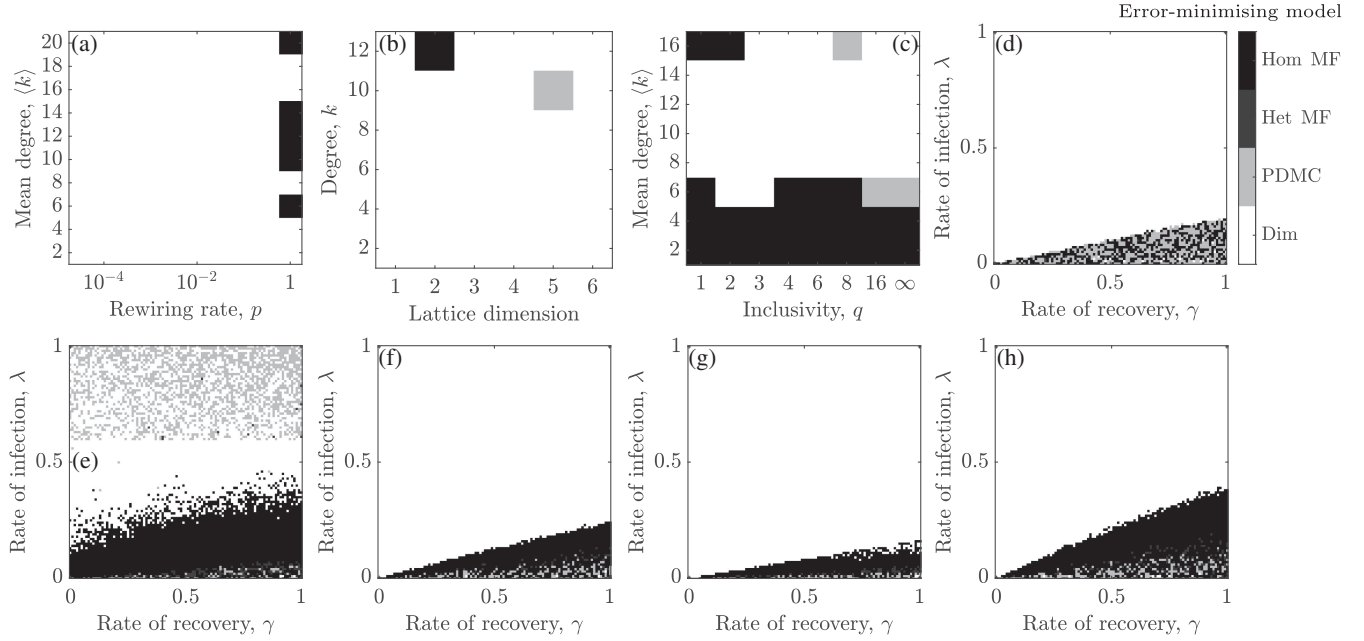
FIG. 3.   The dimensional spreading model leads to lower error than other models across a range of topological and dynamical conditions. Conditions under which each continuous-state model leads to the lowest error in the early spreading stage: homogeneous mean field (black), heterogeneous mean field (dark gray), probabilistic discrete Markov chain (light gray), and dimensional spreading (white). Variation of optimal model with (a) Rewiring rate p and mean degree $\langle k \rangle$ on a small world network with lattice dimension one; (b) Lattice dimension and degree k on a regular lattice; (c) Inclusivity q and mean degree $\langle k \rangle$ on scale-free networks generated via preferential attachment; and rate of infection λ and rate of recovery γ on (d) Two-dimensional lattice; (e) BA scale-free network (53% of points are white, i.e., the dimensional spreading model is optimal for 53% of the considered combinations of parameters); (f) The high school friendship network Friendship II; (g) Erdős collaboration network; and (h) Power grid of the western United States.

other established SIR spreading models (Fig. S5-S6; Sec. V [38]).

For a more systematic comparison of continuous-state models, next we consider a range of topological and dynamical parameters and for each calculate the mean Euclidean error in predictions of the time series $(S(t), I(t), R(t))$, $0 \leq t \leq t_{\max}$. In Fig. 3 we delineate the circumstances in which each spreading model minimizes error. The dimensional spreading model achieves optimal predictions on one-dimensional small world networks across a wide range of mean degree $\langle k \rangle$ and random rewiring rate p, especially for lower p when dimensional structure is more distinct [Fig. 3(a)]. It also offers best performance for regular lattices across a wide range of lattice dimension and degree k [Fig. 3(b)]. For over half of the considered combinations of network model parameters, the proposed model even provides lowest error for scale-free networks generated via preferential attachment across a range of strengths of structural correlation controlled via an "inclusivity" parameter [61] q such that $q = 1$ is maximally correlated and $q = \infty$ corresponds to the minimally correlated BA model [Fig. 3(c)]. Advantages become even clearer if we neglect homogeneous MF and compare only with the more complex methods heterogeneous MF and PDMC: dimensional spreading is then optimal for 94% of considered combinations of network model parameters

(see Supplemental Material [38], Fig. S7). On a range of synthetic and empirical networks the dimensional spreading model is frequently the best performer across a range of values of epidemic parameters, though not for large γ or small λ [Figs. 3(d)–3(h)]. This restriction suggests limitations in the factor a given by Eq. (5), because the small λ and large γ regime is when this term would be most relevant. When the ratio λ/γ is not too small, the reduction in error arising from using the dimensional spreading model is often substantial (see Supplemental Material [38], Fig. S8), and the model frequently offers similar advantages for other values of the epidemic spreading parameters (see Supplemental Material [38], Fig. S9).

Finally, we demonstrate how the proposed basic reproduction number R_0 derived from the dimensional spreading model provides insights about final system state not available from other spreading models. By Eq. (7), $R_0 > \lambda/\gamma$, and to make possible $R_0 \leq 1$ we now employ $\lambda = 0.1$, $\gamma = 0.2$. Once again we consider a range of model parameters, but now for each we determine the average final affected ratio $\tilde{R}(\infty) = (1/N)\lim_{t \to \infty} R(t)$. In Fig. 4 we compare $\tilde{R}(\infty)$ with level sets of R_0 based on each considered continuous-state model. As $\langle k \rangle$, p and lattice dimension vary, $\tilde{R}(\infty)$ changes, but R_0 calculated using the established homogeneous MF, heterogeneous MF and PDMC methods remains almost constant [Figs. 4(a)
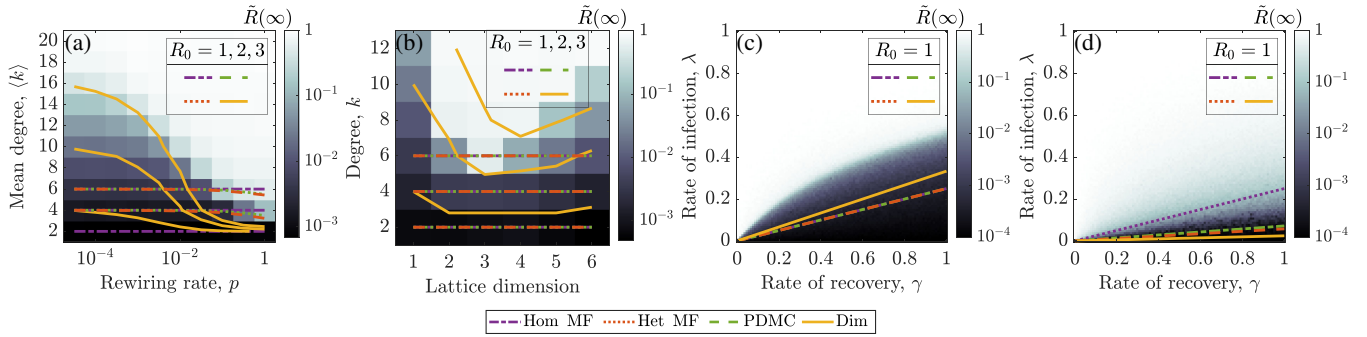
FIG. 4. The basic reproduction number derived from the dimensional spreading model provides information regarding ultimate system state not available from basic reproduction numbers derived from other models. Variation of final affected ratio $\tilde{R}(\infty)$ with (a) Rewiring rate p and mean degree $\langle k \rangle$ on a small world network with lattice dimension one; (b) Lattice dimension and degree k on a regular lattice; and rate of infection λ and rate of recovery γ on (c) Two-dimensional lattice; and (d) BA scale-free network. Curves show level sets of R_0 inferred from the homogeneous mean field (purple dot-dashed), heterogeneous mean field (red dotted), probabilistic discrete Markov chain (green dashed), and proposed dimensional (yellow solid) model.

and 4(b)]. In contrast, R_0 determined from our dimensional spreading model varies meaningfully with topological properties, and its level sets often approximate the level sets of $\tilde{R}(\infty)$. The dimensional spreading model holds similar advantages for epidemic spreading parameters more conducive to spreading (see Supplemental Material [38], Fig. S10) and for the considered scale-free network model (see Ref. [38], Fig. S11). However, regardless of the continuous-state model from which it derived, the basic reproduction number $R_0 \propto \gamma/\lambda$ exhibits the same trends in λ and γ [Figs. 4(c) and 4(d)]; for additional networks see Fig. S12 [38]).

Conclusion.—The global structural correlations typical of real networks lead to systematic errors in important continuous-state models for epidemic spreading. We illustrated how these limitations can be mitigated by taking SIR as an example, although the general approach should also apply to other processes. We proposed a spreading model which depends on topology only through mean degree, network correlation dimension and a constant of proportionality. Relative to established models which are of substantially higher complexity but do not exploit network dimension, our model can predict early stages of the spreading process more accurately and implies a basic reproduction number providing additional information about final system state.

The model's advantage arises from leverage of a global property which can more meaningfully characterize spreading than the local properties on which many established spreading models rely. However, the demonstrated good performance is a nontrivial finding, even for perfect lattices. Our dimensional model relies on representing a system having many state variables with just two scalars, the number infected and number recovered. Given our parsimony with state variables and topological parameters, it is not surprising that the match is imperfect for some networks and sets of epidemic parameters. Nonetheless, the

high performance of this simple model across a wide range of dynamical and topological conditions demonstrates the value of including in spreading models global properties such as dimension.

It would be valuable to apply the dimensional spreading approach to other important spreading processes, such as those separately representing vaccinated, detected and exposed states [5,62], and to other classes of networks, including directed [63], multilayer [64], temporal [65], or perhaps signed [66] networks. In addition, because not all networks have clear dimensional structure, it would be useful to extend it to alternative descriptions for the scaling of network distance [67,68].

[*]haiying.wang@usst.edu.cn

[1] M. Jalili and M. Perc, Information cascades in complex networks, J. Complex Netw. **5**, 665 (2017).
[2] Y. Hu, S. Ji, Y. Jin, L. Feng, H. E. Stanley, and S. Havlin, Local structure can identify and quantify influential global spreaders in large scale social networks, Proc. Natl. Acad. Sci. U.S.A. **115**, 7468 (2018).

[3] H. Wang, J. M. Moore, J. Wang, and M. Small, The distinct roles of initial transmission and retransmission in the persistence of knowledge in complex networks, Appl. Math. Comput. **392**, 125730 (2021).

[4] J. C. Miller and I. Z. Kiss, Epidemic spread in networks: Existing methods and current challenges, Math. Model. Nat. Phenom. **9**, 4 (2014).

[5] A. Reyna-Lara, D. Soriano-Paños, S. Gómez, C. Granell, J. T. Matamalas, B. Steinegger, A. Arenas, and J. Gómez-Gardeñes, Virus spread versus contact tracing: Two competing contagion processes, Phys. Rev. Res. **3**, 013163 (2021).

[6] M. Boguñá, C. Castellano, and R. Pastor-Satorras, Nature of the epidemic threshold for the susceptibleinfected-susceptible dynamics in networks, Phys. Rev. Lett. **111**, 068701 (2013).

[7] A. S. Mata, M. Boguñá, C. Castellano, and R. Pastor-Satorras, Lifespan method as a tool to study criticality in absorbing-state phase transitions, Phys. Rev. E **91**, 052117 (2015).

[8] C. Castellano and R. Pastor-Satorras, Cumulative merging percolation and the epidemic transition of the susceptible-infected-susceptible model in networks, Phys. Rev. X **10**, 011070 (2020).

[9] R. Pastor-Satorras and A. Vespignani, Epidemic spreading in scale-free networks, Phys. Rev. Lett. **86**, 3200 (2001).

[10] M. Boguñá, R. Pastor-Satorras, and A. Vespignani, Absence of epidemic threshold in scale-free networks with degree correlations, Phys. Rev. Lett. **90**, 028701 (2003).

[11] M. J. Keeling, The effects of local spatial structure on epidemiological invasions, Proc. R. Soc. B **266**, 859 (1999).

[12] Y. Wang, D. Chakrabarti, C. Wang, and C. Faloutsos, Epidemic spreading in real networks: an eigenvalue viewpoint, in *Proceedings of the 22nd International Symposium on Reliable Distributed Systems, Florence* (IEEE, New York, 2003), pp. 25–34, https://ieeexplore.ieee.org/document/1238052.

[13] P. Van Mieghem, J. Omic, and R. Kooij, Virus spread in networks, IEEE ACM Trans. Networking **17**, 1 (2008).

[14] S. Gómez, A. Arenas, J. Borge-Holthoefer, S. Meloni, and Y. Moreno, Discrete-time Markov chain approach to contact-based disease spreading in complex networks, Europhys. Lett. **89**, 38009 (2010).

[15] K. J. Sharkey, Deterministic epidemic models on contact networks: Correlations and unbiological terms, Theor. Popul. Biol. **79**, 115 (2011).

[16] A. S. Mata and S. C. Ferreira, Pair quenched mean-field theory for the susceptible-infected-susceptible model on complex networks, Europhys. Lett. **103**, 48003 (2013).

[17] I. Z. Kiss, J. C. Miller, and P. L. Simon, *Mathematics of Epidemics on Networks* (Springer, Cham, 2017), Vol. 598, p. 31.

[18] A. S. Mata, R. S. Ferreira, and S. C. Ferreira, Heterogeneous pair-approximation for the contact process on complex networks, New J. Phys. **16**, 053006 (2014).

[19] J. P. Gleeson, S. Melnik, J. A. Ward, M. A. Porter, and P. J. Mucha, Accuracy of mean-field theory for dynamics on real-world networks, Phys. Rev. E **85**, 026106 (2012).

[20] B. Qu and H. Wang, The accuracy of mean-field approximation for susceptible-infected-susceptible epidemic spreading with heterogeneous infection rates, in *Complex Networks & Their Applications V* (Springer, New York, 2017), pp. 499–510.

[21] L. Hébert-Dufresne and A. Allard, Smeared phase transitions in percolation on real complex networks, Phys. Rev. Res. **1**, 013009 (2019).

[22] H. Wang, J. M. Moore, M. Small, J. Wang, H. Yang, and C. Gu, Epidemic dynamics on higher-dimensional small world networks, Appl. Math. Comput. **421**, 126911 (2022).

[23] A. Safari, P. Moretti, and M. A. Muñoz, Topological dimension tunes activity patterns in hierarchical modular networks, New J. Phys. **19**, 113011 (2017).

[24] M. Small and D. Cavanagh, Modelling strong control measures for epidemic propagation with networks—A COVID-19 case study, IEEE Access **8**, 109719 (2020).

[25] G. Ódor, Nonuniversal power-law dynamics of susceptible infected recovered models on hierarchical modular networks, Phys. Rev. E **103**, 062112 (2021).

[26] H. Sakaguchi and Y. Nakao, Slow decay of infection in the inhomogeneous susceptible-infected-recovered model, Phys. Rev. E **103**, 012301 (2021).

[27] T. Wen, D. Pelusi, and Y. Deng, Vital spreaders identification in complex networks with multi-local dimension, Knowl. Based Syst. **195**, 105717 (2020).

[28] R. Peach, A. Arnaudon, and M. Barahona, Relative, local and global dimension in complex networks, Nat. Commun. **13**, 3088 (2022).

[29] C. Song, S. Havlin, and H. A. Makse, Self-similarity of complex networks, Nature (London) **433**, 392 (2005).

[30] E. Rosenberg, *Fractal Dimensions of Networks* (Springer, Cham, 2020).

[31] J. M. Moore, H. Wang, M. Small, G. Yan, H. Yang, and C. Gu, Correlation dimension in empirical networks, Phys. Rev. E **107**, 034310 (2023).

[32] J. M. Moore, Dim-spread (2024), https://github.com/JackMurdochMoore/dim-spread.git.

[33] H. S. Rodrigues, Application of SIR epidemiological model: New trends, Int. J. Appl. Math. Inf. **10**, 92 (2016), https://www.naun.org/main/UPress/ami/2016/a262013-075.pdf.

[34] Y. Moreno, M. Nekovee, and A. F. Pacheco, Dynamics of rumor spreading in complex networks, Phys. Rev. E **69**, 066130 (2004).

[35] S. Ji, L. Lü, C. H. Yeung, and Y. Hu, Effective spreading from multiple leaders identified by percolation in the susceptible-infected-recovered (SIR) model, New J. Phys. **19**, 073020 (2017).

[36] J. R. C. Piqueira and V. O. Araujo, A modified epidemiological model for computer viruses, Appl. Math. Comput. **213**, 355 (2009).

[37] C. Carroll and T. Wang, Epidemiological expectations, in *Handbook of Economic Expectations* (Elsevier, Amsterdam, 2023), pp. 779–806.

[38] See Supplemental Material at http://link.aps.org/supplemental/10.1103/PhysRevLett.132.237401 for additional text, a table, and figures supporting our results.

[39] O. Diekmann, J. Heesterbeek, and M. G. Roberts, The construction of next-generation matrices for compartmental epidemic models, J. R. Soc. Interface **7**, 873 (2009).

[40] S. Boccaletti, V. Latora, Y. Moreno, M. Chavez, and D.-U. Hwang, Complex networks: Structure and dynamics, Phys. Rep. **424**, 175 (2006).

[41] M. Youssef and C. Scoglio, An individual-based approach to SIR epidemics in contact networks, J. Theor. Biol. **283,** 136 (2011).

[42] D. J. Watts and S. H. Strogatz, Collective dynamics of 'small-world' networks, Nature (London) **393,** 440 (1998).

[43] A.-L. Barabási and M. Pósfai, *Network Science* (Cambridge University Press, Cambridge, 2016).

[44] R. A. Rossi and N. K. Ahmed, The network data repository with interactive graph analytics and visualization, in *Proceedings of the AAAI Conference on Artificial Intelligence, Austin* (AAAI Press, Palo Alto, 2015), pp. 4292–4293, https://ojs.aaai.org/index.php/AAAI/article/view/9277.

[45] P. S. Bearman, J. Moody, and K. Stovel, Chains of affection: The structure of adolescent romantic and sexual networks, Am. J. Sociology **110,** 44 (2004).

[46] H. Ito, K. Shigeta, T. Yamamoto, and S. Morita, Exploring sexual contact networks by analyzing a nationwide commercial-sex review website, PLoS One **17,** e0276981 (2022).

[47] J. Moody, Peer influence groups: identifying dense clusters in large networks, Soc. Networks **23,** 261 (2001).

[48] W. De Nooy, A. Mrvar, and V. Batagelj, *Exploratory Social Network Analysis with Pajek* (Cambridge University Press, Cambridge, England, 2005), https://doi.org/10.1017/CBO9780511806452.

[49] A.-L. Barabási and R. Albert, Emergence of scaling in random networks, Science **286,** 509 (1999).

[50] S. M. Kissler, P. Klepac, M. Tang, A. J. Conlan, and J. R. Gog, Sparking "The BBC Four Pandemic": Leveraging citizen science and mobile phones to model the spread of disease (2018), https://doi.org/10.1101/479154.

[51] J. A. Firth, J. Hellewell, P. Klepac, S. Kissler, A. J. Kucharski, and L. G. Spurgin, Using a real-world network to model localized COVID-19 control strategies, Nat. Med. **26,** 1616 (2020).

[52] A. Cho, J. Shin, S. Hwang, C. Kim, H. Shim, H. Kim, H. Kim, and I. Lee, Wormnet v3: a network-assisted hypothesis-generating server for *Caenorhabditis elegans*, Nucleic Acids Res. **42,** W76 (2014).

[53] J. Leskovec, J. Kleinberg, and C. Faloutsos, Graph evolution: Densification and shrinking diameters, AACM Trans. Knowl. Discover Data **1,** 2 (2007).

[54] F. Brglez, D. Bryan, and K. Kozminski, Combinational profiles of sequential benchmark circuits, in *Proceedings of the 1989 IEEE International Symposium on Circuits and Systems (ISCAS)* (IEEE, New York, 1989), pp. 1929–1934.

[55] K.-I. Goh, M. E. Cusick, D. Valle, B. Childs, M. Vidal, and A.-L. Barabási, The human disease network, Proc. Natl. Acad. Sci. U.S.A. **104,** 8685 (2007).

[56] K. Amunts, C. Lepage, L. Borgeat, H. Mohlberg, T. Dickscheid, M.-É. Rousseau, S. Bludau, P.-L. Bazin, L. B. Lewis, A.-M. Oros-Peusquens, N. J. Shah, T. Lippert, K. Zilles, and A. C. Evans, Bigbrain: An ultra-highresolution 3D human brain model, Science **340,** 1472 (2013).

[57] H. Jeong, S. P. Mason, A.-L. Barabási, and Z. N. Oltvai, Lethality and centrality in protein networks, Nature (London) **411,** 41 (2001).

[58] V. Batagelj and A. Mrvar, Some analyses of Erdős collaboration graph, Soc. Networks **22,** 173 (2000).

[59] B. Rozemberczki, R. Davies, R. Sarkar, and C. Sutton, Gemsec: Graph embedding with self clustering, in *Proceedings of the 2019 IEEE/ACM International Conference on Advances in Social Networks Analysis and Mining, Vancouver* (Association for Computing Machinery, New York, 2019), pp. 65–72, https://doi.org/10.1145/3341161.3342890.

[60] L. E. C. Rocha, F. Liljeros, and P. Holme, Information dynamics shape the sexual networks of internetmediated prostitution, Proc. Natl. Acad. Sci. U.S.A. **107,** 5706 (2010).

[61] J. M. Moore, M. Small, and G. Yan, Inclusivity enhances robustness and efficiency of social networks, Physica (Amsterdam) **563A,** 125490 (2021).

[62] X.-L. Peng, X.-J. Xu, X. Fu, and T. Zhou, Vaccination intervention on epidemic dynamics in networks, Phys. Rev. E **87,** 022813 (2013).

[63] C. Li, H. Wang, and P. Van Mieghem, Epidemic threshold in directed networks, Phys. Rev. E **88,** 062802 (2013).

[64] M. Perc, Diffusion dynamics and information spreading in multilayer networks: An overview, Eur. Phys. J. Spec. Top. **228,** 2351 (2019).

[65] X. Ru, J. M. Moore, X.-Y. Zhang, Y. Zeng, and G. Yan, Inferring patient zero on temporal networks via graph neural networks, in *Proceedings of the AAAI Conference on Artificial Intelligence, New Orleans* (AAAI Press, Washington, DC, 2023), pp. 9632–9640, https://doi.org/10.1609/aaai.v37i8.26152.

[66] H.-J. Li, W. Xu, S. Song, W.-X. Wang, and M. Perc, The dynamics of epidemic spreading on signed networks, Chaos Solitons Fractals **151,** 111294 (2021).

[67] G. Csányi and B. Szendrői, Fractal–small-world dichotomy in real-world networks, Phys. Rev. E **70,** 016122 (2004).

[68] F. Kawasaki and K. Yakubo, Reciprocal relation between the fractal and the small-world properties of complex networks, Phys. Rev. E **82,** 036113 (2010).

Correction: Typographical errors in Eq. (5) and in the paragraph above Eq. (5), in which "max" was used instead of "min," have been set right.